Boosting or Hindering: AoI and Throughput Interrelation in Routing-Aware Multi-Hop Wireless Networks

Jiadong Lou, *Student Member, IEEE*, Xu Yuan, *Member, IEEE*, Sastry Kompella, *Senior Member, IEEE*, and Nian-Feng Tzeng, *Fellow, IEEE*

***Abstract*— While considerable work has addressed the optimal AoI under different circumstances in single-hop networks, the exploration of AoI in multi-hop wireless networks is rarely attempted. More importantly, the inherent relationships between AoI and throughput are yet to be explored, especially in multi-hop networks. This paper studies AoI in multi-hop wireless networks and explores its potential relationships with throughput for the very first time, particularly focusing on the impacts of flexible routes on the two metrics, i.e., AoI and throughput. By developing a rigorous mathematical model with interference, channel allocation, link scheduling, and routing path selection taken into consideration, we build the interrelation between AoI and throughput in multi-hop networks. A multi-criteria optimization problem is formulated with the goal of simultaneously minimizing AoI and maximizing network throughput. By qualitatively analyzing their relationships, we exhibit that the two metrics may conflict with each other, implying the optimal solutions for the multi-criteria problem will include a set of Pareto-optimal points rather than a single point existing in the traditional optimization problem. We resort to a novel approach by transforming the multi-criteria problem into a single objective one so as to find the weakly Pareto-optimal points iteratively, thereby allowing us to screen all Pareto-optimal points for the solution. Through formal proof, our solution is demonstrated to be able to identify all Pareto-optimal points and terminate in a finite number of iterations. We conduct the simulation evaluation to identify the optimal tradeoff points of AoI and throughput, demonstrating that one performance metric may improve at the expense of degrading the other, with the routing path found as one of the key factors in determining such a tradeoff.**

***Index Terms*— Age of Information, network throughput, multi-hop wireless networks, pareto-optimal points.**

I. Introduction

AGE-OF-INFORMATION (AoI) [2], [3] has received growing attention lately due to its prominent advantages of capturing information updating timeliness over the traditional metric of delay. Such a metric of capturing timely updates is deemed absolutely essential for emerging applications in Cyber-Physical Systems (CPS) and Internet of Things (IoT), critically important for punctual responses. Defined as the time elapsed since the generation time of the latest arrival packet at a target destination node, AoI characterizes timely information delivery at the destination, with [3] demonstrating the optimal AoI to be significantly different from the minimized delay. Hence, in contrast to the conventional metrics of delay and throughput, which capture the effectiveness of data collection and transmission for the overall networks (e.g., delay reflects the mean transmission time of all packets), AoI aims to quantify the time-critical updates at a receiver.

To date, AoI in single-hop network has been extensively studied. Efforts have been put in pursuit of AoI optimization by considering packet generation control [2]–[4], various queue management mechanisms [5]–[7], and scheduling policies [8]–[12]. In addition, the multi-access techniques, including ALOHA and Round robin, are considered in [13], [14] to bring AoI into realistic network settings. Moreover, different network environments (e.g., with constraints on interference [15], throughput [16]–[18], and energy [19]) have been studied for AoI optimization under certain constraints. However, the study of AoI in multi-hop networks is rarely attempted although it has gained increasing interests in the ad-hoc network systems, such as smart cities, vehicular communications, weather forecasting, among others, where emerging applications demand urgent responses while the deployed sensors or monitors are scattered across a broad area that is far away from the control center. Prior AoI studies on multi-hop networks limit their scopes to either a special network topology or an abstracted network setting [1], [17], [20]–[22]. For example, [20] dealt with AoI in the gossip network, whereas [21] considered a two-hop network for AoI optimization. In [17], [22], AoI for multi-hop networks with interference constraints was pursued, but its analytic models simplify the network setting by pre-grouping interference-free sets without taking into account the real-world factors of channel allocation, routing, and others.

On the other hand, although AoI has its prominent advantages in characterizing information freshness, the throughput metric, which gauges the network transmission speed, cannot be ignored in AoI exploration. For instance, in a large-scale smart home network, plenty of diverse smart

Manuscript received April 1, 2020; revised December 28, 2020; accepted January 16, 2021; approved by IEEE/ACM TRANSACTIONS ON NETWORKING Editor J. Xie. Date of publication February 24, 2021; date of current version June 16, 2021. This work was supported in part by the NSF under Grant 1948374 and Grant 2019511. This article was presented at the IEEE INFOCOM, Virtual Conference, July 6–9, 2020. *(Corresponding author: Xu Yuan.)*

Jiadong Lou, Xu Yuan, and Nian-Feng Tzeng are with the School of Computing and Informatics, University of Louisiana at Lafayette, Lafayette, LA 70504 USA (e-mail: jiadong.lou1@louisiana.edu; xu.yuan@louisiana.edu; nianfeng.tzeng@louisiana.edu).

Sastry Kompella is with the U.S. Naval Research Laboratory, Washington, DC 20375 USA (e-mail: sastry.kompella@nrl.navy.mil).

Digital Object Identifier 10.1109/TNET.2021.3059694

devices are deployed to gather monitoring information. In such a network, small AoI is crucial to meet timely responses for urgent events and high throughput is also a necessary requirement to handle massive data uploads, besides a higher throughput can support less packet discarding in the waiting queue, which ensures data collection completeness, so as to improve the network performance. An immediate question arises here: Once AoI is optimized at the receiver, will the network throughput be boosted or hindered, especially in multi-hop wireless networks? While [16], [17] have considered the throughput constraint in its pursuit of AoI optimization, the inherent relationship between AoI and throughput is unexplored therein. In [23], authors have discussed the relationship between throughput and AoI in the single-hop network. However, the landscape about relationships between AoI and throughput in the multi-hop network has not been systematically analyzed. Hence, the other existing studies have failed to pursue the optimization of AoI and throughput for exploring their inherent association, especially in multi-hop networks with realistic factors such as channel access modulation, interference, routing path, and others, taking into consideration.

In this paper, we tackle AoI and throughput optimization in routing-aware multi-hop networks for the first time, aiming to explore the inherent relationships of the two metrics, i.e., boosting or hindering one versus the other. In particular, the OFDM-based channel access modulation is employed for the multi-hop networks, and flexible routing paths are considered for each session. By addressing a series of challenges, we characterize the channel allocation, link scheduling, packet generation, and route selection to derive the AoI formula in multi-hop wireless networks. A rigorous model is then developed to interrelate AoI and throughput in multi-hop networks. Given such a model, we formulate a multi-criteria optimization problem with the objectives of simultaneously minimizing AoI and maximizing throughput. By qualitatively analyzing the interrelation of AoI and throughput, these two performance metrics are found to potentially conflict with each other, requiring us to pursue a set of performance tradeoff points (i.e., Pareto-optimal points) to capture the scenarios that AoI boosts or hinders throughput, and vice versa.

To solve the developed multi-criteria problem, which is in the complex form of non-linear and non-convex programming, we develop a novel algorithm for its efficient solution, with an aim at determining all AoI and throughput tradeoff points, i.e., Pareto-optimal points. Specifically, our developed algorithm first transforms the multi-criteria problem into a single objective one, so as to find the weakly Pareto-optimal points iteratively and then to screen Pareto-optimal points for the solution. Since each transformed single objective problem is still in the non-linear form, another algorithm based on the piece-wise linearization technique is then designed to reformulate the non-linear terms approximately into a set of linear segments so that such a single objective problem is solvable by commercial software efficiently. In the end, we formally prove that our developed algorithm can find all Pareto-optimal points in a finite number of iterations. The significance of finding all Pareto-optimal points is that it offers the entire landscape of achievable throughput and AoI tradeoffs, exhibiting the global view of the relationships between them. In contrast, a solution to the traditional problem, such as maximizing throughput under AoI constraints or minimizing AoI under throughput constraints, only represents one point in our solutions. In addition, under certain scenarios where one performance metric (AoI or throughput) has a higher priority than the other one, the network service provider can always find an optimal tradeoff between AoI and throughput instantly from the set of our Pareto-optimal points. Specifically, by assigning certain weights (i.e., priorities) to AoI and throughput, we can simply calculate the weighted values, by subtracting the weighted AoI value from the weighted throughput value, with respect to all Pareto-optimal points. The optimal point results from such assigned weights that yield the maximum value.

We conduct simulation evaluation to quantify AoI and throughput performance with the flexible routes. A case study is presented to show how to find all Pareto-optimal points iteratively and their associated routing paths. The global landscape of AoI and throughput relationships is also presented in our case study, demonstrating that the improvement in one metric is at the expense of deteriorating the other, with the routing path identified as one of the key factors in dictating such a tradeoff between optimal AoI and throughput. Besides, the impacts of other network factors, such as session amounts, interference strength, and routing schemes on such a tradeoff, are also presented in our numerical results.

The remainder of this paper is organized as follows. In Section II, we describe our problem and key challenges. Section III presents the mathematical model and multi-criteria problem formulation for AoI and throughput optimization while Section IV conducts the theoretical analysis of the interrelation of AoI and throughput. In Section V, we develop a novel algorithm to solve the multi-criteria problem with the aim of finding all AoI and throughput tradeoff points. In Section VI, we develop an algorithm based on the piece-wise linearization technique to transform nonlinear terms in the derived single objective problem (given in Section V) into a set of linear segments to make it solvable. In Section VII, we present numerical results. Section VIII outlines related work, Section IX discusses the limitations and future work, and Section X concludes this paper.

II. Problem Description

In wireless networks, both information timeliness and network transmission speed are critical performance metrics, with the former for measuring the information update timeliness and the latter for gauging the network transmission speed. In this paper, we conduct a systematic study of the information update timeliness problem in multi-hop wireless networks and explore its interrelation to the network throughput, aiming to guide network service providers to make intelligent decisions for efficient resource allocations via balancing multiple network performance goals. We consider a multi-hop wireless network comprising of a set of nodes $\mathcal{N}$. Suppose all nodes employ the OFDM channel access modulation for data transmission and a set of $\mathcal{B}$ orthogonal channels (with equal bandwidth) are available for scheduling. There is a

set of sessions $\mathcal{L}$ in this network, where the source and destination nodes of each session $l \in \mathcal{L}$ are denoted as s_l and d_l, respectively. To transport data from a source to its destination, the routing is not pre-fixed, so each session has the flexibility to select the appropriate route so as to meet its transmission needs. Each session corresponds to a time-sensitive application, which requires updates from the source to reach the destination in a timely manner. We take the *Age of Information (AoI)* as the metric of choice to measure information updating timeliness [2], [3]. Meanwhile, the network throughput, which gauges the packet transmission speed, is also an important criterion that should be taken into consideration.

The goal of this paper is to explore the interrelation of AoI and network throughput in OFDM-based multi-hop wireless networks, particularly focusing on the impacts of flexible routes on the two metrics. There are a number of challenges yet to be addressed:

- In multi-hop networks, the packets from source nodes need to traverse multiple relays to reach the destination, making it necessary to model the consecutive transmission behaviors across the intermediate nodes to capture the AoI variation. A new AoI formula has to be derived, but such formula derivation is challenging, especially when the routing paths (i.e., traversed intermediate nodes) are unknown.
- We aim to jointly take such real-world factors as interference, channel allocation schemes, scheduling, routing paths and others into considerations for characterizing the AoI formula in multi-hop networks. Such a joint consideration of real-world factors is rarely attempted even in single hop networks, letting alone incorporating them into the study of AoI optimization in multi-hop networks.
- The intricate interrelation of AoI and throughput brings more difficulty in our exploration. It is necessary yet challenging to identify the polar relationships of these two metrics (i.e., boosting or hindering them) and develop the suitable solutions accordingly to find the optimal AoI and throughput.

III. Mathematical Modeling and Problem Formulation

In this section, we develop a mathematical model to characterize the inherent relationships of AoI and throughput in routing-aware multi-hop networks. To develop such a model, the rigorous AoI formula will be derived in multi-hop networks, capturing the impact of resource allocations, link scheduling, interference and routing paths. A multi-criteria problem is then formulated for simultaneously optimizing AoI and throughput. The developed mathematical modeling and problem formulation will address the challenges outlined in the last section through a joint formulation.

A. Network Model

Let $\mathcal{T}_i$ denote the set of nodes in $\mathcal{N}$ located within a node i's transmission range. Since the route for each session is not pre-fixed, i may choose any node in its transmission range to relay its transported data. We let a binary variable $n_{ij}^l[b]$ indicate if a link (i,j) is set up (i.e., activated) in a channel b for a session l as follows: $n_{ij}^l[b] = 1$ $(i \in \mathcal{N}, j \in \mathcal{T}_i)$ if the link (i,j) is activated in channel $b \in \mathcal{B}$ for a session $l \in \mathcal{L}$; $= 0$, otherwise.

1) Interference Constraints: Assume that all sessions are unicast, i.e., node i can receive from or transmit to only one node in a channel, we have:

$$\sum_{l\in\mathcal{L}}\sum_{j\in\mathcal{T}_i} n_{ij}^l[b] \le 1, \quad (i \in \mathcal{N}, b \in \mathcal{B}). \tag{1}$$

$$\sum_{l\in\mathcal{L}}\sum_{k\in\mathcal{T}_i} n_{ki}^l[b] \le 1, \quad (i \in \mathcal{N}, b \in \mathcal{B}). \tag{2}$$

To account for half-duplex at each node, we have:

$$\sum_{l\in\mathcal{L}} n_{ij}^l[b] + \sum_{l\in\mathcal{L}} n_{ki}^l[b] \le 1, \ (i \in \mathcal{N}, j,k \in \mathcal{T}_i, b \in \mathcal{B}). \tag{3}$$

The above unicast and half-duplex constraints (1), (2), and (3) can be replaced equivalently by the following constraint:

$$\sum_{l\in\mathcal{L}}\sum_{j\in\mathcal{T}_i} n_{ij}^l[b] + \sum_{l\in\mathcal{L}}\sum_{k\in\mathcal{T}_i} n_{ki}^l[b] \le 1, \ (i \in \mathcal{N}, b \in \mathcal{B}). \tag{4}$$

To model interference among activated links, we consider the interference avoidance among all links. We take into account the protocol interference model, which has been demonstrated to perform similarly as the physical interference model when the interference range is properly set up [24], in order to make our model more tractable. Denote $\mathcal{I}_i$ as the set of nodes located within the interference range of a node $i \in \mathcal{N}$, we have:

$$\sum_{l\in\mathcal{L}} n_{ij}^l[b] + \sum_{l\in\mathcal{L}} n_{ph}^l[b] \le 1, \tag{5}$$

where $i \in \mathcal{T}_j, p \in \mathcal{I}_j, h \in \mathcal{T}_p, j \in \mathcal{N}, j \neq h$, and $b \in \mathcal{B}$. This means if a node j is receiving on channel b, it shall not be interfered on the same channel by an unintended transmitter p that locates within j's interference range.

2) Link Activation Frequency: Let f_{ij}^l denote the activation frequency, which indicates the number of channels used to transmit packets of a link (i,j) for session l. We have:

$$f_{ij}^l = \sum_{b\in\mathcal{B}} n_{ij}^l[b], \quad (i \in \mathcal{N}, l \in \mathcal{L}, j \in \mathcal{T}_i). \tag{6}$$

Let binary variable z_{ij}^l represent if a link (i,j) is set up for session l, yielding: $z_{ij}^l = 1$ if $f_{ij}^l \ge 1$; $= 0$, otherwise.

This means if a link (i,j) is set up only if the activation frequency of this link for session l is no less than 1. This statement can be reformulated mathematically into the following forms:

$$f_{ij}^l \ge z_{ij}^l, \quad (1 - z_{ij}^l) f_{ij}^l < 1. \tag{7}$$

3) Routing Constraints: Suppose there is only one path for each session and the paths from different sessions can intersect at some nodes. To consider the network connectivity of each session and avoid heavy congestion among different sessions, we assume no multiple paths, share the same link. The routing path for each session $l \in \mathcal{L}$ is flexible and is considered as an optimization variable, we have:

- If node i is the source of a session l, we have:

$$\sum_{j \in \mathcal{T}_i} z_{ij}^l = 1 \ , \quad (i = s_l). \tag{8}$$

- If node i is an intermediate node for a session l, we have:

$$\sum_{j \in \mathcal{T}_i, j \neq s_l} z_{ij}^l = \sum_{k \in \mathcal{T}_i, k \neq d_l} z_{ki}^l \ , \quad (i \neq s_l, i \neq d_l). \tag{9}$$

- If node i is the destination node of a session l, we have:

$$\sum_{k \in T_i} z_{ki}^l = 1 \ , \quad (i = d_l). \tag{10}$$

Since no link is shared by multiple sessions, we define two other variables f_{ij} and z_{ij} as $f_{ij} = \sum_{l \in \mathcal{L}} f_{ij}^l$ and $z_{ij} = \sum_{l \in \mathcal{L}} z_{ij}^l$. Then, we have:

$$z_{ij} \leq 1 \ , \quad (i \in \mathcal{N}, j \in \mathcal{T}_i) \ . \tag{11}$$

4) Packet Transmission Model: Assuming that source nodes in all sessions are always working to produce updates, and each of them divides or adapts the generated data into packets of a uniform size, denoted as p^l for source node of a session l. Notably, we allow variation of packet sizes in different sessions. Denote λ^l as the generation rate at source s_l of session l, then the time interval of packet generation at the sender s_l is the constant $\frac{1}{\lambda^l}$.

Let μ_{ij}^l denote the transmission rate of link (i, j) for delivering packet of session l, with the rate constrained by the total link capacity. We have:

$$\mu_{ij}^l \leq f_{ij} C_{ij}, \tag{12}$$

where f_{ij} is the link activation frequency of all sessions and C_{ij} accounts for the link capacity in a link (i, j). We have:

$$C_{ij} = W_B \log_2(1 + \frac{P_i d_{ij}^{-\gamma}}{N_0}), \tag{13}$$

where W_B is the bandwidth of each channel b, p_i the power spectral density from transmitter i, d_{ij} the distance between nodes i and j, γ the path loss index, and N_0 the ambient Gaussian noise density.

When the network reaches the steady-state, to avoid the packet loss caused by the infinite number of backlogged packets at any relay node, the transmission time of each packet on a link should be no larger than the packet generation time interval of the session that employs it. We have the following constraint:

$$\frac{1}{\lambda^l} \geq \frac{p^l}{\mu_{ij}^l}, \tag{14}$$

for the active link (i, j). Since no link is shared with multiple sessions, this can be reformulated as follows:

$$\mu_{ij}^l \geq \sum_{l \in \mathcal{L}} \lambda^l p^l z_{ij}^l. \tag{15}$$

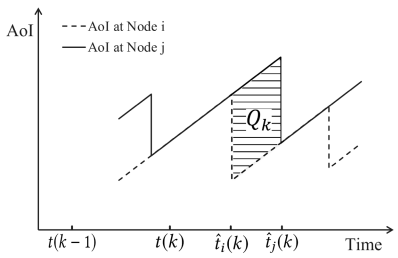

Fig. 1. AoI variation at two consecutive nodes.

5) Throughput Model: To facilitate our exploration of inherent AoI and throughput relationships, in this paper, all packets are assumed to be always delivered successfully to destination nodes eliminating the probability events. Within a time range $(0, T)$, the throughput of session l (denoted as U^l) can be expressed as:

$$U^l = \frac{K p^l}{T} = \lambda^l p^l, \tag{16}$$

where K is the total number of packets generated within $(0, T)$ for this session. Hence, the constraint (15) can be rewritten as:

$$\mu_{ij}^l \geq \sum_{l \in \mathcal{L}} U^l z_{ij}^l. \tag{17}$$

B. AoI Formula

Let $D_{d_l}(t)$ indicate the generation time of the latest packet reaching the destination node $d_l, l \in \mathcal{L}$. The instantaneous AoI at time t, denoted by $a_{d_l}(t)$, is calculated by $a_{d_l}(t) = t - D_{d_l}(t)$. Based on the graphical argument, the total aggregated AoI, denoted as ΔA_{d_l}, over time range $(0, T)$ at a destination node d_l can be calculated by the area under the curve of instantaneous AoI, i.e.,

$$\Delta A_{d_l} = \int_0^T a_{d_l}(t) dt. \tag{18}$$

Then, the time averaged AoI at the destination node d_l (denoted as A_{d_l}) in time range $(0, T)$ is expressed by:

$$A_{d_l} = \frac{1}{T} \int_0^T a_{d_l}(t) dt. \tag{19}$$

To model AoI in the multi-hop networks, we first find the AoI relationships of two consecutive nodes and then derive AoI at a destination node recursively. Let A_i^l and A_j^l denote the time averaged AoI at a node i and its successor node j for the packets from a session $l \in \mathcal{L}$. We have:

Lemma 1: If a link (i, j) is set up between node i and node j, time averaged AoIs for packets (from the same source node s_l) at these two nodes satisfy the following relationship:

$$A_j^l = A_i^l + \frac{p^l}{\mu_{ij}}. \tag{20}$$

Proof: The proof is based on the graphical approach. As shown in Figure 1, the kth packet is generated at time $t(k)$ and reaches node i and node j at time $\hat{t}_i(k)$ and $\hat{t}_j(k)$, respectively. Assume a packet arriving at a node can be transmitted to its

successor node immediately without considering the propagation delay. Here, the dashed and solid lines represent the AoI at nodes i and j, respectively. The difference of the aggregated AoIs at nodes i and j during time $(0, T)$ equals the sum of shadow parallelogram parts labeled in Figure 1. We have:

$$\Delta A_j^l = \Delta A_i^l + \sum_{k=1}^{K} Q_k, \tag{21}$$

where K is the number of packets delivered within the time span of $(0, T)$ and Q_k is the area of kth parallelogram. From Figure 1, the area Q_k is expressed as the product of $\hat{t}_j(k) - \hat{t}_i(k)$ and $t(k) - t(k-1)$, which are the transmission time of a packet via link (i, j) and the packet generation interval, respectively. Hence, (21) can be given by

$$\Delta A_j^l = \Delta A_i^l + \sum_{k=1}^{K} \frac{1}{\lambda^l} \frac{p^l}{\mu_{ij}}. \tag{22}$$

Then, we have the time averaged AoI at node j within $(0, T)$ as follows:

$$\begin{aligned} A_j^l &= \frac{1}{T}\Big(\Delta A_i^l + \sum_{k=1}^{K} \frac{1}{\lambda^l} \frac{p^l}{\mu_{ij}}\Big) \\ &= A_i^l + \frac{K}{T} \frac{\sum_{k=1}^{K} \frac{1}{\lambda^l} \frac{p^l}{\mu_{ij}}}{K} \\ &= A_i^l + \frac{p^l}{\mu_{ij}}, \end{aligned} \tag{23}$$

where the term $\frac{K}{T}$ is equal to the packet generation rate λ^l. □

The importance of Lemma 1 is that it enables us to recursively derive the time averaged AoI at a destination node d_l iteratively starting from the source node s_l.

Theorem 1: Time averaged AoI at the destination node $d_l, l \in \mathcal{L}$, can be calculated by:

$$A_{d_l} = \frac{1}{2\lambda^l} + \sum_{i \neq d_l, z_{ij}^l = 1} \frac{p^l}{\mu_{ij}}, \tag{24}$$

where j is i's successor node and $z_{ij}^l = 1$ represents that link (i, j) is set up for transmitting packets over session l.

Proof: Based on Lemma 1, time averaged AoI at the destination node d_l can be calculated iteratively from the source node s_l's successor node a (where $z_{s_l a}^l = 1$). Hence, we have:

$$A_{d_l} = A_a^l + \sum_{i \neq d_l, i \neq s_l, z_{ij}^l = 1} \frac{p^l}{\mu_{ij}}. \tag{25}$$

Here, $z_{ij}^l = 1$ represents that link (i, j) is set up for transmitting packets over session l. From Figure 2, the aggregated AoI at the node a for session l, denoted by ΔA_a^l, equals the sum of trapezoid parts, accounting the area difference between two isosceles right triangles. Hence, we have:

$$\Delta A_a^l = \sum_{k=1}^{K} \{\frac{1}{2}[\hat{t}(k) - t(k-1)]^2 - \frac{1}{2}[\hat{t}(k) - t(k)]^2\}, \tag{26}$$

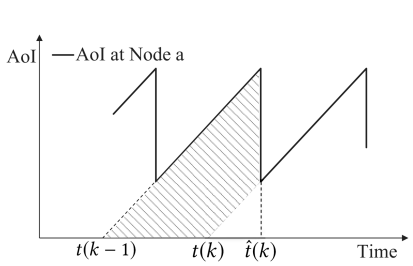

Fig. 2. AoI variation at node a, the successor of source node s_l.

where K is the number of packets delivered to node a. In Figure 2, the kth packet is generated at time $t(k)$ and received by node a at $\hat{t}(k)$. The term of $t(k) - t(k-1)$ is the time interval of packets generation, which equals $\frac{1}{\lambda^l}$, and the term $\hat{t}(k) - t(k)$ is the packet transmission time, which equals $\frac{p^l}{\mu_{s_l a}}$. As a result, the aggregated AoI can be calculated by:

$$\begin{aligned} \Delta A_a^l &= \sum_{k=1}^{K} \{\frac{1}{2}[\hat{t}(k) - t(k-1)]^2 - \frac{1}{2}[\hat{t}(k) - t(k)]^2\} \\ &= \sum_{k=1}^{K} [\frac{1}{2}(\frac{1}{\lambda^l} + \frac{p^l}{\mu_{s_l a}})^2 - \frac{1}{2}(\frac{p^l}{\mu_{s_l a}})^2] \\ &= \sum_{k=1}^{K} (\frac{1}{2{\lambda^l}^2} + \frac{p^l}{\lambda^l \mu_{s_l a}}). \end{aligned} \tag{27}$$

Thus, time averaged AoI at node a over $(0, T)$ is:

$$\begin{aligned} A_a^l &= \frac{1}{T} \sum_{k=1}^{K} (\frac{1}{2{\lambda^l}^2} + \frac{p^l}{\lambda^l \mu_{s_l a}}) \\ &= \frac{K}{T} \frac{1}{K} \sum_{k=1}^{K} (\frac{1}{2{\lambda^l}^2} + \frac{p^l}{\lambda^l \mu_{s_l a}}) \\ &= \lambda^l (\frac{1}{2{\lambda^l}^2} + \frac{p^l}{\lambda^l \mu_{s_l a}}) \\ &= \frac{1}{2\lambda^l} + \frac{p^l}{\mu_{s_l a}}. \end{aligned} \tag{28}$$

where the term $\frac{K}{T}$ is the packet generation rate λ^l of session l. Combining (28) and (25), we have:

$$\begin{aligned} A_{d_l} &= A_a^l + \sum_{i \neq d_l, i \neq s_l}^{z_{ij}^l = 1} \frac{p^l}{\mu_{ij}} \\ &= \frac{1}{2\lambda^l} + \frac{p^l}{\mu_{s_l a}} + \sum_{i \neq d_l, i \neq s_l}^{z_{ij}^l = 1} \frac{p^l}{\mu_{ij}} \\ &= \frac{1}{2\lambda^l} + \sum_{i \neq d_l, z_{ij}^l = 1} \frac{p^l}{\mu_{ij}}. \end{aligned}$$

□

From (24), we can see that the first term is related to packet generation interval while the second term comes from the transmission delay over multiple traversed links on a specified session route. Such an AoI formula exhibits that the minimization of AoI in multi-hop wireless networks is a comprehensive work involving the generation rate control,

channel allocation, link scheduling, interference, the routing selection, and the delay management.

Denote A^{ave} as the time averaged AoI of all sessions, then

$$A_{ave} = \sum_{l\in\mathcal{L}} A_{d_l} = \sum_{l\in\mathcal{L}}(\frac{1}{2\lambda^l} + \sum_{i\neq d_l}^{z_{ij}^l=1} \frac{p^l}{\mu_{ij}}) = \sum_{l\in\mathcal{L}} \frac{1}{2\lambda^l} + \sum_{i\in\mathcal{N}} \sum_{j\in\mathcal{T}_i}^{z_{ij}^l=1} \frac{p^l}{\mu_{ij}}. \quad (29)$$

C. Problem Formulation

Our developed model aims to both maximize throughput and minimize AoI. For throughput, we are interested in maximizing the minimum throughput (denoted as $U_{\min}$) among all sessions, i.e.,

$$U_{\min} = \min\{U^l, l \in \mathcal{L}\}. \quad (30)$$

Then, it can be rewritten as the following constraint:

$$U_{\min} \leq U^l, \quad l \in \mathcal{L}, \quad (31)$$

Our problem can be formulated as a multi-criteria optimization problem with the objectives of minimizing AoI and maximizing throughput across all sessions. That is,

$$\begin{aligned} \text{OPT} \quad & \min \ A_{ave} \\ & \max \ U_{\min} \\ & s.t. \text{ The total time averaged AoI function: } (29); \\ & \quad \text{Interference constraints: } (4),\ (5); \\ & \quad \text{Links activation frequency: } (7); \\ & \quad \text{Routing constraints: } (8),\ (9),\ (10),\ (11); \\ & \quad \text{Transmission model: } (12),\ (17); \\ & \quad \text{Throughput model: } (16),\ (31). \end{aligned}$$

From OPT, we observe that the solution for the optimal throughput may not lead to the minimal achievable AoI value as each of them wishes to find the best resource allocation and routing solutions for optimality individually. The next section will analyze the relationships of those two metrics in multi-hop wireless networks.

IV. Qualitative Analysis of AoI and Throughput Relationships

In this section, we provide the qualitative analysis of relationships between AoI and throughput, especially under the flexible routing, aiming to guide our algorithm design for solving the problem OPT. One question will be answered in our analysis: whether these two metrics can be always optimized at the same time? In the following analysis, we will consider two potential network scenarios, and examine the AoI and throughput variations to discuss the condition that optimizes the two metrics.

We first analyze the relationship of the two objectives under the given routes. For ease of explanation, we take only one session in multi-hop networks as an example and assume that there is a known route in which the AoI has achieved the global minimum. Under the solution of achieving such an optimal AoI, denote links' capacity among all channels as $\{f_1C_1, f_2C_2, \cdots, f_nC_n\}$. Without loss of generality, we assume $f_1C_1 \leq f_2C_2 \leq \cdots \leq f_nC_n$. According to the constraint (17), the maximum throughput is limited by f_1C_1.

To examine whether the AoI and throughput have arrived at their optimum at the same time, we can check whether the throughput can continue to improve. In the multi-hop route, it is possible to have the following condition to be satisfied:

$$(f_k - 1)C_k > f_1C_1, \quad k \in \{2, 3, \cdots, n\}. \quad (32)$$

If this condition holds, even in the worse case where link 1 interferes with all other links, there still exists a new channel allocation solution which can lead the links' capacity to be: $\{(f_1 + 1)C_1, (f_2 - 1)C_2, \cdots, (f_n - 1)C_n\}$. Hence, we can arrive a larger throughput value with the new bottleneck link capacity of $(f_1 + 1)C_1$. As the channel allocation solution has been changed, the AoI may deteriorate. Our extensive experiments have exhibited this condition holds in the majority of our studies. One example will be also presented in our case study (Figures 5(a) and 5(c) in Section VII-A). This indicates that the throughput has the opportunity to increase at the expense of AoI performance by altering channel allocations results. Thus, we conclude that these two metrics may conflict, hindering both of them concurrently achieving the optimal values in the case of a fixed route.

We next check whether we can change the routing path to increase the achievable throughput. According to (13), we observe that the link capacity and the link length have the following relationships: $C_{ij} \propto log(d_{ij}^{-\gamma})$. Hence, the link capacity increases with decreasing of the distance d_{ij}. When optimizing AoI, we did not target to minimize the distance of two neighboring nodes, thus it is possible existing other routes that have shorter lengths for the bottleneck links, which can achieve better throughput performances. However, since the current AoI has achieved its minimum value, the change of route may deteriorate AoI performance. Our experiments also confirms that this is the general case in the multi-hop networks. Our case study in Section VII-A will exhibit the examples that shortening bottleneck links will improve the network throughput but degrading the AoI performance.

Although our aforementioned analysis is intuitive and may not be general enough to accommodate all network settings, its results give us the hints that AoI and throughput often are not optimized concurrently under typical network environments. In contrast, they may conflict with each other sometimes. Thus, the traditional optimization solutions toward obtaining a single optimal solution cannot be applied here. Instead, we have to develop a uniform solution that can adopt both scenarios, i.e., the two objectives boost or hinder each other. This inherently brings the difficulty for us to develop the suitable algorithm to solve the problem OPT. In the next section, we will design an algorithm toward finding the

Pareto-optimal point(s) that can include both scenarios to represent the optimal tradeoff of AoI and throughput.

V. Algorithm Design for AoI and Throughput Tradeoffs

In this section, we aim to simultaneously minimize AoI and maximize throughput by pursuing the *Pareto-optimal points* to exhibit their tradeoffs. The goal of our design is to develop an algorithm that finds all Pareto-optimal points, corresponding to all optimal solutions, for the multi-objective problem OPT. Notably, for the scenario that AoI and throughput conflict with each other, multiple Pareto-optimal points will exist. If the two objectives boost with each other, i.e., achieving the global optimal solution at the same time, only one Pareto-optimal point will appear, which is a special case in our designed algorithm.

A. Background for Pareto-Optimal Solution

A Pareto-optimal point is a state of resource allocation where neither objective can be improved without deteriorating the other. The solution corresponding to a Pareto-optimal point is called the *Pareto-optimal solution*. For a Pareto-optimal solution ϕ^*, if the objective pair $(A^*_{ave}, U^*_{\min})$ is *a Pareto-optimal point*, there is no other feasible solution ϕ with the objective pair $(A_{ave}, U_{\min})$ such that $A_{ave} < A^*_{ave}$ and $U_{min} \geq U^*_{\min}$, or $A_{ave} \leq A^*_{ave}$ and $U_{\min} > U^*_{\min}$. This means it is impossible to find another solution to make AoI lower without degrading throughput, or to increase throughput without deteriorating AoI. Besides, an objective pair $(\tilde{A}_{ave}, \tilde{U}_{\min})$ to the solution $\tilde{\phi}$ is a *weakly Pareto-optimal point* if there does not exist a solution ϕ with $A_{ave} < \tilde{A}_{ave}$ and $U_{\min} > \tilde{U}_{\min}$. It is apparent that a Pareto-optimal point is also a weakly Pareto-optimal point whereas a weakly Pareto-optimal point is not always a Pareto-optimal point.

B. Finding a Weakly Pareto-Optimal Point

In this section, we provide a two-step approach for determining a weakly Pareto-optimal point. First, we reformulate OPT into a single AoI objective problem by adding a new throughput constraint v while removing the throughput objective function. This problem is reformulated as follows:

OPT-AoI

$$\min \ A_{ave}$$

$$s.t. \text{ Throughput constraint: } U_{\min} > v,$$

$$\text{Constraints: } (4), (5), (7)-(12), (16), (17), (29), (31).$$

By solving this problem, we get an optimal AoI value (denoted as A^v_{ave}) with a routing solution (denoted as $\mathbf{R}^v$). Notably, OPT-AoI is in the form of mixed-integer nonlinear programming, which cannot be solved directly. Our developed linearized algorithm (elaborated in Section VI) is applied here to linearize the non-linear terms in the objective function into a set of linear segments to make OPT-AoI solvable by commercial solvers.

Second, we find the maximum throughput under solution $\mathbf{R}^v$, denoted as U_{R^v}. Based on (16) and (29), we have:

$$\begin{aligned} A_{ave} &= \sum_{l\in\mathcal{L}} \frac{1}{2\lambda^l} + \sum_{i\in\mathcal{N}} \sum_{j\in\mathcal{T}_i}^{z^l_{ij}=1} \frac{p^l}{\mu_{ij}} \\ &= \sum_{l\in\mathcal{L}} \frac{p^l}{2U^l} + \sum_{i\in\mathcal{N}} \sum_{j\in\mathcal{T}_i}^{z^l_{ij}=1} \frac{p^l}{\mu_{ij}}. \end{aligned} \tag{33}$$

Let $\mathcal{H}(\mathbf{R}, \mathbf{U}) = A_{ave}$, where $\mathbf{R} = \{\mathbf{n}, \mathbf{f}, \mathbf{z}, \mu\}$ represents resource allocation solutions and $\mathbf{U} = \{U^l | l \in \mathcal{L}\}$ represents the throughput solutions. For a given route and the channel allocation of selected links, for each session l, we have:

$$\frac{\partial \mathcal{H}}{\partial U^l} = -\frac{p^l}{2{U^l}^2} \leq 0. \tag{34}$$

It indicates that AoI decreases as throughput increases until both of them reach the optimal values. However, based on constraints (17) and (12), the throughput with a known route is limited to the bottleneck link's capacity for the avoidance of the unbound delay caused by infinite queuing at some relay nodes. Let U_R denote the maximum throughput achievable under certain solution $\mathbf{R}$. We have:

$$U_R = \min_{z^l_{ij}=1} \{f_{ij} C_{ij}\}, \tag{35}$$

where $z^l_{ij} = 1$ indicates the link (i, j) is in the known route of l. This means, once the route and its channel allocation scheme are known, AoI and throughput can achieve their local optimal values simultaneously and the throughput is limited to the value of U_R.

Based on Eqn. (35), we can obtain the optimal throughput, i.e., U_{R^v}, under the solution of OPT-AoI.

Lemma 2: The objective pair (A^v_{ave}, U_{R^v}) is a weakly Pareto-optimal point.

Proof: The proof is based on contradiction. Assume that the pair (A^v_{ave}, U_{R^v}) is not a weakly Pareto-optimal point. There must be a solution ϕ' with an objective pair $(A^{v'}_{ave}, U'_{R^v})$, that satisfies $A^{v'}_{ave} < A^v_{ave}$ and $U'_{R^v} > U_{R^v}$. Since $U'_{R^v} > U_{R^v} > v$, ϕ' is a feasible solution to problem OPT-AoI. However, given A^v_{ave} is the minimum value in this problem, we have $A^{v'}_{ave} \geq A^v_{ave}$, contradicting the assumption. □

Since a Pareto-optimal point is also a weakly Pareto-optimal point, if we find all weakly Pareto-optimal points, all Pareto-optimal points are then be included.

C. Determining All Pareto-Optimal Points

This subsection provides an algorithm to determine all Pareto-optimal points. While Section V-B describes how to find a weakly Pareto-optimal point with a constant v, there is an infinite number of values for v, making it impractical to traverse all v values to identify all weakly Pareto-optimal points. We provide an effective approach for selecting some v values simply based on those weakly Pareto-optimal points found, instead of arbitrarily searching for all v values. The essence of our algorithm is to jump the routing path from one

Algorithm 1 Finding Pareto-Optimal Points

Step 1:
Initialization: $v = 0, M = 0, P = (0, 0)$, an empty set $\mathcal{O}$.
Solve OPT-AoI with the parameter v.
Step 2:
while Existing feasible solution to OPT-AoI with the parameter v. **do**
Step 2.1:
Record the objective value A^v_{ave} and the routing R^v.
Calculate U_{R^v} based on (35).
Add the point $P = (A^v_{ave}, U_{R^v})$ to $\mathcal{O}$.
Step 2.2:
if $A^v_{ave} = M$ **then**
Remove the point P from $\mathcal{O}$.
end if
Step 2.3:
$M = A^v_{ave}$ and $v = U_{R^v}$.
Solve OPT-AoI with the parameter v.
end while

to another by adjusting the values of v, with the following general idea. In each iteration, an OPT-AoI problem is solved with a throughput constraint v to find an optimal value of AoI. The maximum throughput can be calculated based on the current solution. Hence, we get a weakly Pareto-optimal pair and then set v as the current maximum throughput value for the next iteration. By comparing the AoI values, we single out all Pareto-optimal points among those weakly Pareto-optimal points found. Algorithm details are shown in Algorithm 1.

Theorem 2: The set $\mathcal{O}$ from Algorithm 1 includes all Pareto-optimal points and the algorithm terminates in a finite number of iterations.

Proof: The proof consists of three steps. We first show that each objective pair in $\mathcal{O}$ is a Pareto-optimal point. Based on Lemma 2, each objective pair (A^v_{ave}, U_{R^v}) is a weakly Pareto-Optimal point. **Step 2.2** in Algorithm 1 is the screening procedure of Pareto-optimal points among the weakly Pareto-optimal points. Consider two objective pairs, denoted respectively by (A^a_{ave}, U_{R^a}) and (A^b_{ave}, U_{R^b}), and suppose the pair (A^b_{ave}, U_{R^b}) is found in the iteration after (A^a_{ave}, U_{R^a}). Since the parameter v is always equal to the throughput found in the last iteration and the throughout keeps increasing, the solution of A^b_{ave} for OPT-AoI is also a feasible solution for A^a_{ave}, yielding $A^a_{ave} \leq A^b_{ave}$. In Algorithm 1, any weakly Pareto-optimal point with the same AoI value as that of the next point is dropped from the set $\mathcal{O}$, so $A^a_{ave} < A^b_{ave}$. As $U_{R^b} > U_{R^a}$ and $A^a_{ave} < A^b_{ave}$, we conclude that any two consecutive points in $\mathcal{O}$ are Pareto-optimal points.

Next, we prove that all Pareto-optimal points are found by Algorithm 1. This has to show that at each iteration, there is no more Pareto-optimal point whose throughput value is bigger than that found in the previous iteration (denoted as (A^p_{ave}, U_{R^p})) and is smaller than that derived in the current iteration (denoted as (A^c_{ave}, U_{R^c})).

This is proved by contradiction. Suppose there is a Pareto-optimal point (A'_{ave}, U') satisfying the above assumption, then $U_{R^p} < U' \leq U_{R^c}$. As $U' \leq U_{R^c}$, the point (A'_{ave}, U') can be a Pareto-optimal point only if $A'_{ave} < A^c_{ave}$, giving rise to improved AoI. Based on the assumption of $U_{R^p} < U'$, the objective pair (A'_{ave}, U') is also a feasible solution for problem OPT-AoI with the throughput constraint of $U > U_{R^p}$. Since A^c_{ave} is the optimal value under this constraint, we have $A'_{ave} \geq A^c_{ave}$. This contradicts to $A'_{ave} < A^c_{ave}$. Thus, there is no other Pareto-optimal point existing between two neighboring ones.

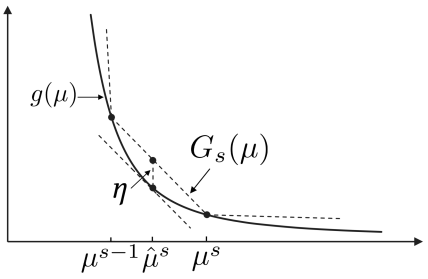

Fig. 3. The piece-wise approximation of $\frac{1}{\mu}$ with linear segments within the approximate error η.

Finally, we show that Algorithm 1 terminates in a finite number of iterations. Since the activation frequency is an integer variable in range $(0, |\mathcal{B}|)$ and C_{ij} has at most $\mathcal{N}^2$ different values, based on (35), the numbers of viable U_{R^v} and of v values are at most $|\mathcal{B}| \cdot |\mathcal{N}|^2$. Besides, from the throughput constraint in problem OPT-AoI and **Step 2.3** in Algorithm 1, the value of throughput threshold v increases with each iteration. Hence, Algorithm 1 terminates in a finite number of iterations. □

VI. Linearization of OPT-AoI

The last section outlines a solution for determining all Pareto-optimal points iteratively for the multi-criteria problem of OPT. However, in each iteration, a single objective problem OPT-AoI needs to be solved to find a corresponding weakly Pareto-optimal point. As OPT-AoI is in the form of non-linear non-convex programming, we apply the piece-wise linearization technique to transform the problem of OPT-AoI into mixed-integer linear programming (MILP), so that it can be directly solved by commercial software.

A. Linearization of $\frac{1}{\mu}$

A nonlinear part of OPT-AoI lies in the objective function, i.e., $\frac{1}{\mu_{ij}}$ in (33). With $g(x) = \frac{1}{x}$, the objective function then can be replaced by:

$$A_{ave} = \sum_{l \in \mathcal{L}} \frac{p^l}{2U^l} + p^l \sum_{i \in \mathcal{N}} \sum_{j \in \mathcal{T}_i}^{z^l_{ij}=1} g(\mu_{ij}).$$

As $\frac{\partial g(\mu)}{\partial \mu^2} = \frac{2}{\mu^3} > 0$, $g(\mu)$ proved to be a convex function. This allows us to employ the piece-wise linearization technique to approximate the curve of $g(\mu)$ with a set of linear segments while ensuring the gap between the value of any point on $g(\mu)$ and that on the corresponding linear segments to stay within an approximate error η as shown in Figure 3.

We denote the minimum value of μ as $C^{\min}$, which is C_{ij} of the bottleneck link among all sessions. Since the maximum

Algorithm 2 Piece-Wise Linearization

Initialization: $s = 1$ and $\mu^{s-1} = C^{min}$.
while $\mu^{s-1} < |\mathcal{B}|C^{max}$ **and** $g(\mu^{s-1}) > \eta$ **do**
  Calculate slop q^s by solving (38).
  With q^s, calculate μ^s based on (36).
  $s = s + 1$.
end while
if $\mu^{s-1} \geq |\mathcal{B}|C^{max}$ **then**
  $S = s - 1, \mu^S = |\mathcal{B}|C^{max}$, and recalculate q^S based on (36).
else if $g(\mu^{s-1}) \leq \eta$ **then**
  $S = s, \mu^S = |\mathcal{B}|C^{max}$, and calculate q^S based on (36).
end if

value of f_{ij} is $|\mathcal{B}|$, μ is upper bounded by $|\mathcal{B}|C^{\max}$ (from (12)), where $C^{\max}$ is the maximum value of C_{ij} among all links. Assuming that the minimum number of linear segments is S, μ^0 is the X-axis value for the start point, and $\mu^1, \mu^2 \cdots, \mu^S$ are the X-axis values for the end points of linear segments, we have $\mu^0 = C^{\min}$ and $\mu^S = |\mathcal{B}|C^{\max}$.

To ensure the minimum number of S, we start to calculate the slope of the first segment from μ^0 and ensure the approximate gap between this linear segment and the original curve to be no more than η. With this start point and the slope, we obtain the end point of this segment that intersects with the original curve and treat it as the start point of the second segment, denoted by μ^1. We repeat the above process until finding adequate segments that cover the entire feasible range of μ. Denoting the s-th linear segment and its slope as $G_s(\mu)$ and q^s, respectively, we have:

$$q^s = \frac{g(\mu^s) - g(\mu^{s-1})}{\mu^s - \mu^{s-1}}, \tag{36}$$

$$G_s(\mu) = q^s \cdot (\mu - \mu^{s-1}) + g(\mu^{s-1}). \tag{37}$$

Within each range of (μ^{s-1}, μ^s), there is a point with the maximum gap between the linear segment and the curve, denoted as η. If the x-coordinate of that point is denoted by $\hat{\mu}^s$, we have:

$$\frac{\partial g(\hat{\mu}^s)}{\partial \mu} - q^s = 0,\ G_s(\hat{\mu}^s) - g(\hat{\mu}^s) = \eta. \tag{38}$$

The slope q^s can be obtained by solving above equations. If for the start point of the s-th segment with $g(\mu^{s-1}) \leq \eta$, we set its end point at $\mu^s = |\mathcal{B}|C^{max}$ and then have the last segment drawn from $(\mu^{s-1}, g(\mu^{s-1}))$ to $(|\mathcal{B}|C^{max}, g(|\mathcal{B}|C^{max}))$. Algorithm 2 gives the details of finding the values of $\mu^1, \cdots, \mu^S$ and slopes $q^1, \cdots, q^S$ for any given approximate error η,

Lemma 3: The approximation error within each linear segment derived from Algorithm 2 is no more than η.

The proof is based on the aforementioned construction process and is omitted here. With Algorithm 2, we can approximate $\frac{1}{\mu}$ in the objective function via a set of linear segments with an error upper bounded by η.

B. Linearization of $\frac{1}{U}$

Similarly, the non-linear part for throughput in the objective function of OPT-AoI also appears in the $g(x)$ form, i.e., $\frac{1}{U^l}$. We follow the same piece-wise linearization solution as above to reformulate it into a set of linear segments with a guaranteed approximate error, denote by η_2. Specifically, it determines the minimum number of linear segments E, the slopes $q_u^1, q_u^2, \ldots, q_u^E$, the X-axis values $U^0, U^1, U^2 \ldots, U^E$ of the linear segments.

C. Problem Reformulation and Approximate Gap

Let $G(\mu)$ and $G_2(U)$ represent the concatenated linear segments for $\frac{1}{\mu}$ and $\frac{1}{U}$, respectively, derived from Sections VI-A and VI-B. The objective $\min A_{ave}$ of OPT-AoI can be replaced by the following linear function and constraints:

$$\min \quad A_{ave}^L$$

$$\text{s.t.} \quad A_{ave}^L = \frac{p^l}{2} \sum_{l \in \mathcal{L}} G_2(U^l) + p^l \sum_{i \in \mathcal{N}} \sum_{j \in \mathcal{T}_i}^{z_{ij}^l = 1} G(\mu_{ij}), \tag{39}$$

$$G(\mu_{ij}) \geq q^s \cdot (\mu_{ij} - \mu^{s-1}) + g(\mu^{s-1}),$$
$$G_2(U^l) \geq q_u^e \cdot (U^l - U^{e-1}) + g(U^{e-1}),$$
$$(s = 1, 2, \cdots, S, \mu \in [C^{min}, |\mathcal{B}|C^{max}]),$$
$$(e = 1, 2, \cdots, E, U \in [0, |\mathcal{B}|C^{max}]). \tag{40}$$

Then, the original OPT-AoI problem is reformulated into the following new optimization problem, i.e.,

$$\text{OPT-L} \quad \min \ A_{ave}^L$$
$$s.t. \text{ Throughput constraint: } U_{min} > v,$$
$$\text{Constraints: } (4), (5), (7) - (12), (16), (17),$$
$$(29), (31), (39), (40).$$

OPT-L is in the form of mixed integer linear programming, which can be solved by commercial solvers (e.g., CPLEX [25]) efficiently. The following theorem characterizes the error bound between the optimal objective values of OPT-L and those of the original OPT-AoI problem.

Theorem 3: The gap between the optimal objective values of OPT-AoI and those of OPT-L, ϵ, is upper bounded by:

$$\frac{p^l}{2} \sum_{l \in \mathcal{L}} \eta_2 + p^l \sum_{i \in \mathcal{N}} \sum_{j \in \mathcal{T}_i}^{z_{ij}^l = 1} \eta. \tag{41}$$

Proof: Suppose the optimal solution of OPT-AoI is $\varphi_{AoI}^* = \{n_{ij}^*[b], f_{ij}^*, z_{ij}^*, \mu_{ij}^*, U^{l^*}\}$ with the objective value being A_{ave}^{O*}. Because the solution φ_{AoI}^* meets all constraints in OPT-L, we can construct a feasible solution (denoted as φ_{AoI-L}) with its n, f, z, μ and U values kept the same as those in φ_{AoI}^* of $G(\mu)$ and $G_2(U)$. Denoting the objective value of the solution φ_{AoI-L} as A_{ave}^L, we have:

$$\begin{aligned} A_{ave}^L - A_{ave}^{O*} &= \frac{p^l}{2} \sum_{l \in \mathcal{L}} G_2(U^{l^*}) + p^l \sum_{i \in \mathcal{N}} \sum_{j \in \mathcal{T}_i}^{z_{ij}^l = 1} G(\mu_{ij}^*) \\ &\quad - \frac{p^l}{2} \sum_{l \in \mathcal{L}} g(U^{l^*}) - p^l \sum_{i \in \mathcal{N}} \sum_{j \in \mathcal{T}_i}^{z_{ij}^l = 1} g(\mu_{ij}^*) \\ &\leq \frac{p^l}{2} \sum_{l \in \mathcal{L}} \eta_2 + p^l \sum_{i \in \mathcal{N}} \sum_{j \in \mathcal{T}_i}^{z_{ij}^l = 1} \eta, \end{aligned}$$

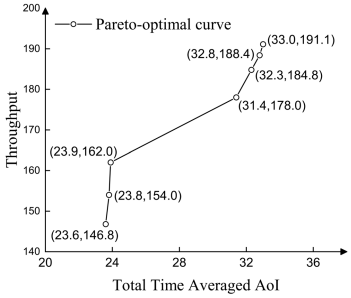

Fig. 4. The Pareto-optimal points found by our Algorithm.

where the last inequality is derived from Lemma 3. Let $\epsilon = \frac{p^l}{2}\sum_{l\in\mathcal{L}}\eta_2 + p^l\sum_{i\in\mathcal{N}}\sum_{j\in\mathcal{T}_i}^{z_{ij}=1}\eta$ and φ^*_{AoI-L} denote the optimal solution of OPT-L, with the objective value of A^{L*}_{ave}. Since A^L_{ave} is the value of a feasible solution to OPT-L, we have $A^{L*}_{ave} \leq A^L_{ave}$. As a result, $A^{L*}_{ave} - A^{O*}_{ave} \leq A^L_{ave} - A^{O*}_{ave} \leq \epsilon$. □

Note that (29), (7), and (17) of OPT-L also include the non-linear terms. Those terms can either be reformulated through Reformulation Linearization Technique (RLT) [26], [27], or be automatically linearized by using the boolean expression in the CPLEX solver with great efficiency.

Our complete solution for OPT-AoI is summarized as follows: for a pre-defined approximate error ϵ, we first can calculate the linearization errors η and η_2 and then construct a set of linear segments based on Algorithm 2. After that, we reformulate OPT-AoI into OPT-L, which is solved by CPLEX.

VII. Numerical Results

In this section, we present the numerical results of AoI and throughput performance in multi-hop networks with flexible routing paths. Our goal is twofold. First, we illustrate how our algorithm identifies the AoI and throughput tradeoff, and show the impact of routing paths on such tradeoffs. Second, we reveal the achievable AoI and throughput curves under different network settings in multi-hop networks.

A. A Case Study

We randomly generate a 25-node network in a 100×100 area. For generality, we normalize the units for distance, bandwidth, power, packet generation, and transmission rate with appropriate dimensions. For demonstrating the impact of routing on the optimal throughput and AoI tradeoff, we take one session as an example for ease of explanation, as depicted in Fig. 5, where the location of each node is shown, so are the source and destination nodes. Assume that there are 15 available channels, each with the bandwidth of 10. The transmission power spectral density of each node i is 10, the pass loss index γ is 4, and the ambient Gaussian noise density equals $N_0 = 10^{-6}$. The node transmission and interference ranges are 35 and 55, respectively. The packet size p is 1000 among all sessions. We set the approximate error $\epsilon = 0.1$ in the linearization algorithm.

According to the above setting, Algorithm 1 executes a total of 7 iterations, in which all resultant points are Pareto-optimal points. In the first iteration, by setting the throughput constraint $v = 0$ and solving the problem of OPT-AoI, we get the minimum value of AoI equal to 23.6, with its associated route marked in Fig. 5(a). The maximum throughput found here is 146.8, giving rise to the first AoI and throughput tradeoff pair of $(23.6, 146.8)$. After this iteration, we set v to the current maximum throughput of 146.8 and continue to run our algorithm. Repeating the above process, our algorithm then returns another six Pareto-optimal points: $(23.8, 154.0)$, $(23.9, 162.0)$, $(31.4, 178.0)$, $(32.3, 184.8)$, $(32.8, 188.4)$, and $(33.0, 191.1)$. Fig. 4 illustrates all AoI and throughput tradeoff points. The routing paths corresponding to all those Pareto-optimal points are shown in Figs. 5(a) to (g).

Table I shows the transmission rate of each link in the routing path of each iteration, with the bottleneck link marked with "$\surd$". We indicate link numbers as $1, 2, \cdots$, from the left to right of each route in Fig. 5. From this table, we can see the throughput increases due to lifting the transmission rate of the bottleneck link from iteration 1 to iteration 7. This is done by either introducing multiple links with shorter distances or by re-arranging the channel allocation scheme. For example, from Fig. 5(a) to Fig. 5(b), the routing path is changed to the one with a shorter averaged link distance, from 26.27 down to 25.86, as shown in Table I, resulting in the throughput increases from 146.8 to 154.0. The AoI performance degrades with such a throughput increase. Similar cases also happen in Fig. 5 from (c) to (d), (d) to (e), and (e) to (f). On the other hand, comparing Fig. 5(a) and Fig. 5(c), we observe that the routing paths appear to be the same. From Table I, we can see in the first iteration (corresponding to Fig. 5(a)), the third link is the bottleneck link with the transmission rate of 146.8 and in the third iteration (corresponding to Fig. 5(c)), link 2 becomes the bottleneck with the transmission rate of 162.0, due to the change of channel allocation scheme. Such a change makes AoI degrade from 23.6 to 23.9. A similar channel allocation change also happens from Fig. 5(f) to Fig. 5(g). These results conform to the conditions discussed in our analysis of Section IV.

From those AoI and throughput performance results, we see that one performance metric improves at the expense of degrading the other, with the routing path found as one of the key factors in determining such a tradeoff. As shown in Table I, we can observe that the averaged transmission rate decreases from 267.5 to 213.8 when the number of hops increases from 5 to 7. In this study case, the minimum AoI is achieved with the fewest-hop path due to the reason that more hops involve more intermediate nodes and lower mean transmission rates, to lengthen the transmission delay and thus heighten AoI.

From Fig. 5 we observe that the trend for lifting the throughput of the session is to increase the number of hops (while worsening AoI). The reason is that by increasing the hop count of a route, the distance between two neighboring nodes decreases, thus exponentially heightening the transmission capacity of their corresponding link accordingly.

B. Comparative Results

We next examine the impact of a certain network setting in multi-hop networks on the optimal AoI and throughput tradeoff.

TABLE I

TRANSMISSION RATE OF LINKS IN EVERY ITERATION AND THE AVERAGED LINK DISTANCES IN EACH ROUTE, WITH THE BOTTLENECK LINK MARKED

Transmission Rate	Link 1	Link 2	Link 3	Link 4	Link 5	Link 6	Link 7	Averaged Rate	Averaged Link Distance
Iteration 1	213.6	202.5	146.8($\surd$)	181.8	593	–	–	267.5	26.27
Iteration 2	282.6	160	154($\surd$)	181.8	474.4	–	–	250.6	25.86
Iteration 3	213.6	162($\surd$)	183.5	181.8	474.4	–	–	243.1	26.27
Iteration 4	178($\surd$)	206.4	184.8	183.5	381.5	216.8	–	225.2	22.03
Iteration 5	188.4	254.8	194	184.8($\surd$)	232.8	197.6	314.8	221.3	20.97
Iteration 6	188.4($\surd$)	254.8	193.8	210	232.8	197.6	236.1	216.2	20.56
Iteration 7	235.5	191.1($\surd$)	193.8	210	232.8	197.6	236.1	213.8	20.56

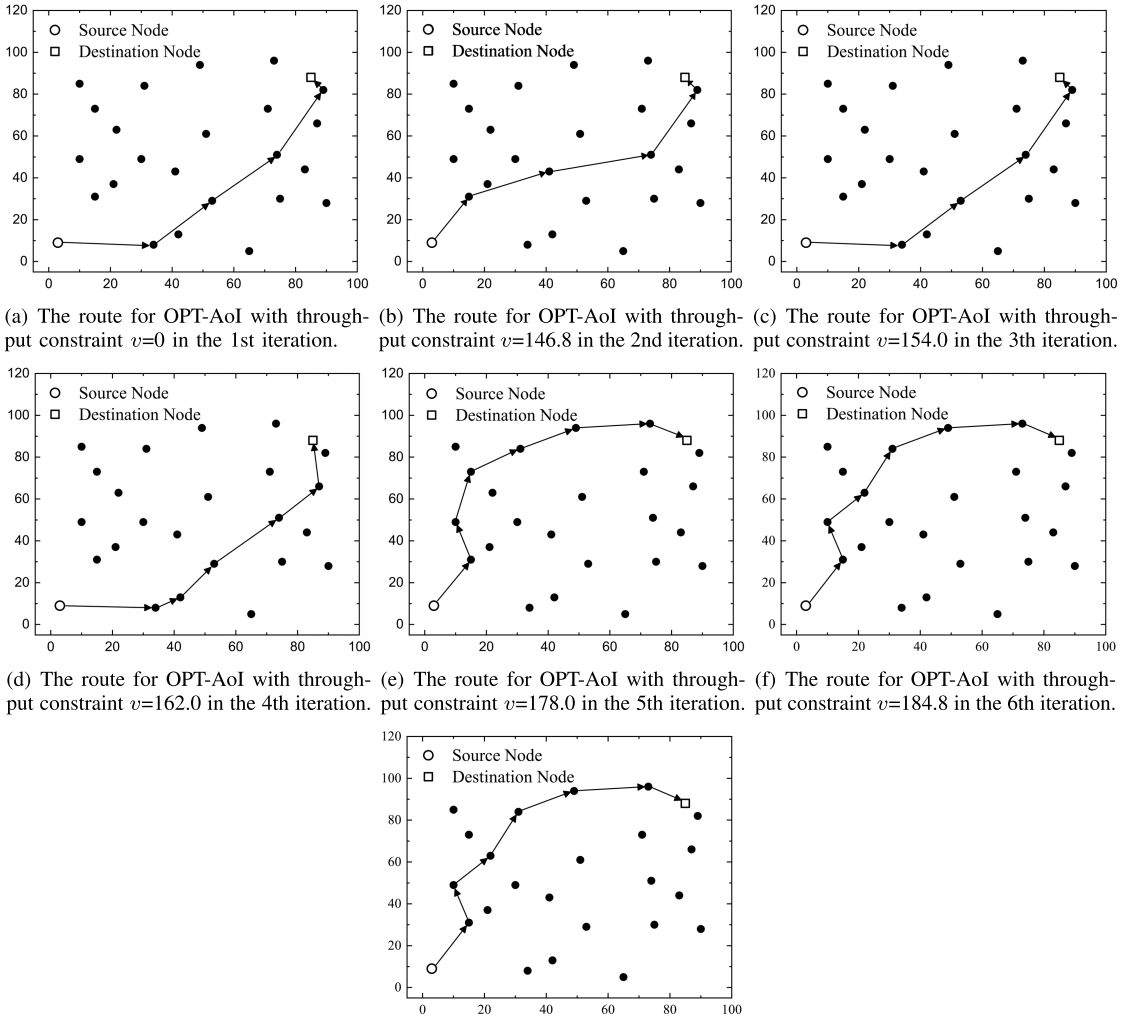

(a) The route for OPT-AoI with throughput constraint v=0 in the 1st iteration.

(b) The route for OPT-AoI with throughput constraint v=146.8 in the 2nd iteration.

(c) The route for OPT-AoI with throughput constraint v=154.0 in the 3th iteration.

(d) The route for OPT-AoI with throughput constraint v=162.0 in the 4th iteration.

(e) The route for OPT-AoI with throughput constraint v=178.0 in the 5th iteration.

(f) The route for OPT-AoI with throughput constraint v=184.8 in the 6th iteration.

(g) The route for OPT-AoI with throughput constraint v=188.4 in the 7th iteration.

Fig. 5. The routes of different AoI and throughput tradeoff points.

Impact of Session Amounts. We first consider various numbers of sessions in the networks. We follow the similar network setting as in Section VII-A and increase the number of sessions to 2, 3, and 5. Fig. 6 shows the optimal throughput and AoI curves (by connecting all Pareto-optimal points) under different numbers of sessions. From this figure, optimal AoI is seen to drop with an increase in the maximum throughput value. This demonstrates the importance of exploring AoI and throughput relationships when studying AoI in the network. In addition, both AoI and throughput deteriorate as the session count in the networks rises. The reason is that more sessions occupy more network resources, thus suffering from higher interference in the network. The resource allocated to each session drops, thereby resulting in larger AoI and lower throughput.

Impact of Interference Strength. We next unveil the impact of interference ranges on the AoI-throughput curve. We randomly generate 3 sessions and vary the interference range from 50, 60, to 70, with AoI-throughput curves depicted in Fig. 7. It is seen that both AoI and throughput deteriorate

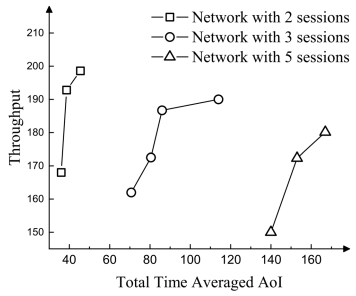

Fig. 6. The AoI and throughput tradeoff with different numbers of sessions.

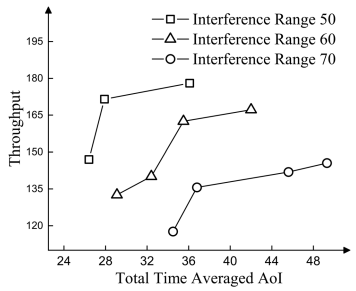

Fig. 7. The AoI and throughput tradeoff with different interference ranges.

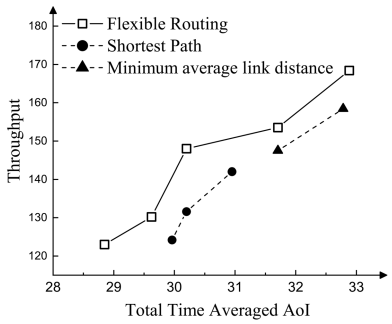

Fig. 8. The AoI and throughput tradeoff under different routing schemes.

with an increase in the interference range as expected, because a larger interference range results in a lower average activation frequency among links. Thus, throughput drops as the result of a lower bottleneck link transmission rate, and AoI rises with a longer transmission time.

Comparison with Different Routing Schemes. We now fix the number of nodes as 25 and generate a single session to explore the impact of routing selection on our solution. As there exist no prior solutions exploring the routing and AoI-throughput tradeoff in multi-hop networks, we take the shortest path and the minimum averaged link distance schemes into consideration for comparison, with the results depicted in Fig. 8. By comparing three Pareto-optimal curves, we see our flexible routing solution to achieve the best in both throughput and AoI. This demonstrates the advantage of our proposed flexible routing scheme. Meanwhile, the shortest path scheme exhibits better AoI while the minimum averaged link distance scheme enjoys higher network throughput, when comparing two of them. The reason is that the former involves fewer relay nodes to yield less transmission delay, thus leading to lower AoI. The latter results in larger averaged link capacity, helping to lift the throughput. However, more relay nodes involved in this scheme heighten AoI.

VIII. Related Work

The conception of AoI was first proposed in [2], [3] as a node perspective metric to measure the data freshness and has received wide attention recently. Extensive works have studied the AoI optimization in single-hop network settings. For instance, generation rate control was studied in [2], in which authors mathematically calculated the optimal generation rate with the First Come First Served (FCFS) policy to optimize AoI at the destination. Later on, the study was extended to the network setting with multiple sources [3]. Besides, the zero-wait policy, in which the source node starts transmitting a new update once the previous one is delivered to the destination, has been proved to worsen AoI in [4]. Such work implies that minimizing AoI may conflicts with maximizing throughput, which results from the zero-wait scheduling policy.

In addition, various queuing packet management methods have been pursued in [5]–[7], where their analyses have demonstrated the similar results that discarding old packets can help improve the data freshness. Moreover, the scheduling policies have been examined for AoI reduction. [8] considered the Last Generated First Served (LGFS) queue scheduling with/without preemption. The AoI variations under preemptive LGFS have been explored under multi-server single-hop networks in [9] and replication techniques with the LGFS policy have been considered for further AoI improvement [10]. Besides, the LGFS policy has been extended to the Max-Age-First LGFS in [11]. All these works merely considered simple network settings and controls without taking into account the impacts of the real-world factors.

Recent studies expand the AoI analysis scope in the single-hop network with different practical settings. The channel access techniques, such as ALOHA and Round Robin, were considered, with [14] employing the slotted ALOHA to schedule packet transmission for minimizing AoI and [13], [14] adopting the "take turns" method for scheduling multiple terminals to communicate with one BS. Meanwhile, different network environments and practical constraints were also considered. The interference among links was addressed in [15] and energy-consuming and harvesting were studied for AoI optimization in [19]. Reference [28] addressed the AoI optimization problem in the scenario where a central station and a set of terminals exchange their data via a mobile agent in order to provide the optimal path for the agent. Reference [29] considered the request and response behavior that accounts for the data freshness of only users' requests.

The throughput was considered for optimal AoI scheduling earlier in [16], [17]. However, it is only set to be a constraint with its value being greater or less than a constant value, to demonstrate the importance of exploring both AoI and throughput at the same time. The landscape view of the inherent relationship between AoI and throughput was unexplored therein. In [23], the authors mentioned the relationship between throughput and AoI in the single-hop network,

knowing that the studied problem becomes more challenging in analyzing multi-hop environments. Reference [18] explored the tradeoff (Pareto-optimal solutions) between the throughput of two clients or the AoI of two clients independently, but it failed to address the relationship between AoI and throughput, especially in the multi-hop networks.

Some studies targeted the AoI optimization problem in multi-hop networks. Specifically, [20] and [21] performed AoI analyses under the special network topologies, with [20] dealing with the gossip networks with nodes connected as line or star topologies, and [21] adopting a sampling policy to optimize AoI in two-hop networks while considering the energy-harvesting nodes. The network in which each source node takes turns to broadcast its information to other nodes was pursued in [30]. Then, authors in [31] showed that the LGFS scheduling policy can help improve the AoI in multi-hop networks under the arbitrary packet generation and arrival times, but the formula of AoI and its achievable values were not provided. None of prior studies accounts for the real-world factors such as interference among links, route selection, and multi-access techniques, thus significantly simplifying the network models. Although [22] has considered the interference constraint in the multi-hop networks and offered the optimal link activation scheduling mechanism based on their previous work [15], its models simplify the network setting by pre-grouping interference-free sets without providing the actual channel access modulation. Notably, our work is utterly different from all previous studies since we provide the general multi-hop model while considering the common real-world factors including interference, channel allocation, link scheduling, link capacity, and routing path selection. Then, we explore the relationships between AoI and throughput in such general multi-hop wireless networks for the very first time, with the impact of flexible routing taking into account.

IX. Discussion

Some limitations exist for this presented work, as stated in sequence below.

First, this work considers the multi-hop network setting where multiple sessions may intersect at some nodes but may not share the same link. The main concern comes from queuing and scheduling issues which result from the multi-source problem at each shared link, since packets that arrive at the link from different sources may follow distinct distributions to behave irregularly. Hence, it is critical on how to schedule the transmission of packets from different sources at the intermediate nodes in the multi-hop settings. The new analysis of the queuing management and scheduling strategies in such a scenario is needed, exhibiting as an open and challenging problem.

Second, this work assumes that all packets can be delivered successfully to destination nodes. It is challenging to consider transmission failures in the multi-hop flexible routing. Compared to the single-hop settings, where a transmission failure can be directly modeled by the assigned success probability at links, however, multi-hop networks have to account for the dilemma that transmission failures can happen at all traversed links. Even if we can model the transmission success probability for entire routes, the modeling for such transmission failures results in a considerable computational expenditure in the multi-hop scenario, due to flexible routing with many potential combinations of links for constructing routes. Consequently, a new analysis of the queuing management, scheduling strategies, and transmission failures in such a scenario is needed. We defer this exploration to our future work.

Third, our simulation outcomes have revealed that routing plays a significant role in the tradeoff between AoI and throughput, and our case studies show insights that routing with fewer traversed nodes is to better improve the AoI but hinder the throughput. Because of the heavy complexities of the modeled multi-criteria optimization problem, we cannot mathematically confirm our findings with solid proofs. Our future work will make effort on refining our network modeling and deepening our analysis of routing influence on these two metrics.

X. Conclusion

Although AoI has been widely explored in the research community, its study in multi-hop networks and its relationships with other performance metrics are not well addressed yet. This paper presented an in-depth study on the optimal AoI and throughput tradeoff in multi-hop networks for the first time, with such physical factors as channel allocation, scheduling, and flexible routing selection taken into consideration. A rigorous mathematical model has been developed to characterize the interrelation of AoI and throughput. By formulating a multi-objective problem and exploring their relationships, we have developed a novel algorithm to find Pareto-optimal point(s) to identify all tradeoff point(s) of the optimal AoI and throughput, covering the network scenarios where AoI and throughput boost and hinder with each other. Our algorithm has been proved to find all Pareto-optimal points with a small number of iterations. The simulation results have demonstrated the existence of a tradeoff between AoI and throughput, with one performance metric improved at the expense of degrading the other. Our mathematical development, algorithmic solutions, and results included in this paper shed light on wireless network design by relating two key performance metrics, calling for AoI and throughput optimization simultaneously, instead of optimizing solely one metric individually.

References

[1] J. Lou, X. Yuan, S. Kompella, and N.-F. Tzeng, "AoI and throughput tradeoffs in routing-aware multi-hop wireless networks," in *Proc. IEEE Conf. Comput. Commun. (INFOCOM)*, Jul. 2020, pp. 476–485.

[2] S. Kaul, R. Yates, and M. Gruteser, "Real-time status: How often should one update?" in *Proc. IEEE Int. Conf. Comput. Commun. (INFOCOM)*, Mar. 2012, pp. 2731–2735.

[3] R. D. Yates and S. K. Kaul, "The age of information: Real-time status updating by multiple sources," *IEEE Trans. Inf. Theory*, vol. 65, no. 3, pp. 1807–1827, Mar. 2019.

[4] Y. Sun, E. Uysal-Biyikoglu, R. Yates, C. E. Koksal, and N. B. Shroff, "Update or wait: How to keep your data fresh," in *Proc. 35th Annu. IEEE Int. Conf. Comput. Commun. (INFOCOM)*, Apr. 2016, pp. 1–9.

[5] M. Costa, M. Codreanu, and A. Ephremides, "Age of information with packet management," in *Proc. IEEE Int. Symp. Inf. Theory*, Jun. 2014, pp. 1583–1587.

[6] M. Costa, M. Codreanu, and A. Ephremides, "On the age of information in status update systems with packet management," *IEEE Trans. Inf. Theory*, vol. 62, no. 4, pp. 1897–1910, Apr. 2016.
[7] N. Pappas, J. Gunnarsson, L. Kratz, M. Kountouris, and V. Angelakis, "Age of information of multiple sources with queue management," in *Proc. IEEE Int. Conf. Commun. (ICC)*, Jun. 2015, pp. 5935–5940.
[8] S. K. Kaul, R. D. Yates, and M. Gruteser, "Status updates through queues," in *Proc. 46th Annu. Conf. Inf. Sci. Syst. (CISS)*, Mar. 2012, pp. 1–6.
[9] A. M. Bedewy, Y. Sun, and N. B. Shroff, "Optimizing data freshness, throughput, and delay in multi-server information-update systems," in *Proc. IEEE Int. Symp. Inf. Theory (ISIT)*, Jul. 2016, pp. 2569–2573.
[10] A. M. Bedewy, Y. Sun, and N. B. Shroff, "Minimizing the age of information through queues," *IEEE Trans. Inf. Theory*, vol. 65, no. 8, pp. 5215–5232, Aug. 2019.
[11] Y. Sun, E. Uysal-Biyikoglu, and S. Kompella, "Age-optimal updates of multiple information flows," in *Proc. IEEE IEEE Conf. Comput. Commun. Workshops (INFOCOM WKSHPS)*, Apr. 2018, pp. 136–141.
[12] J. Lou, X. Yuan, and N.-F. Tzeng, "Instant AoI optimization in IoT networks with packet combination," in *Proc. 17th Annu. IEEE Int. Conf. Sens., Commun., Netw. (SECON)*, Jun. 2020, pp. 1–9.
[13] R. D. Yates and S. K. Kaul, "Status updates over unreliable multiaccess channels," in *Proc. IEEE Int. Symp. Inf. Theory (ISIT)*, Jun. 2017, pp. 331–335.
[14] Z. Jiang, B. Krishnamachari, S. Zhou, and Z. Niu, "Decentralized status update for age-of-information optimization in wireless multiaccess channels," in *Proc. Inf. Theory Appl. Workshop (ITA)*, Feb. 2018, pp. 2276–2280.
[15] R. Talak, S. Karaman, and E. Modiano, "Optimizing information freshness in wireless networks under general interference constraints," in *Proc. 18th ACM Int. Symp. Mobile Ad Hoc Netw. Comput.*, Jun. 2018, pp. 61–70.
[16] I. Kadota, A. Sinha, and E. Modiano, "Optimizing age of information in wireless networks with throughput constraints," in *Proc. IEEE Conf. Comput. Commun.*, Apr. 2018, pp. 1844–1852.
[17] N. Lu, B. Ji, and B. Li, "Age-based scheduling: Improving data freshness for wireless real-time traffic," in *Proc. 18th ACM Int. Symp. Mobile Ad Hoc Netw. Comput.*, Jun. 2018, pp. 191–200.
[18] I. Kadota, "Transmission scheduling of periodic real-time traffic in wireless networks," Ph.D. dissertation, Massachusetts Inst. Technol., Cambridge, MA, USA, 2016.
[19] R. D. Yates, "Lazy is timely: Status updates by an energy harvesting source," in *Proc. IEEE Int. Symp. Inf. Theory (ISIT)*, Jun. 2015, pp. 3008–3012.
[20] J. Selen, Y. Nazarathy, L. L. H. Andrew, and L. V. Hai, "The age of information in gossip networks," *Environ. Technol.*, vol. 27, no. 8, pp. 863–873, 2013.
[21] A. Arafa and S. Ulukus, "Age-minimal transmission in energy harvesting two-hop networks," in *Proc. IEEE Global Commun. Conf. (GLOBECOM)*, Dec. 2017, pp. 1–6.
[22] R. Talak, S. Karaman, and E. Modiano, "Minimizing age-of-information in multi-hop wireless networks," in *Proc. 55th Annu. Allerton Conf. Commun., Control, Comput. (Allerton)*, Oct. 2017, pp. 486–493.
[23] I. Kadota, E. Uysal-Biyikoglu, R. Singh, and E. Modiano, "Minimizing the age of information in broadcast wireless networks," in *Proc. 54th Annu. Allerton Conf. Commun., Control, Comput. (Allerton)*, Sep. 2016, pp. 844–851.
[24] Y. Shi, Y. T. Hou, J. Liu, and S. Kompella, "Bridging the gap between protocol and physical models for wireless networks," *IEEE Trans. Mobile Comput.*, vol. 12, no. 7, pp. 1404–1416, Jul. 2013.
[25] X. Nodet. (2019). *Multiobjective Optimization for LP and MIP in CPLEX*. [Online]. Available: https://developer.ibm.com/docloud/blog/2019/03/12/multiobjective-optimization-for-lp-and-mip-in-cplex/
[26] H. D. Sherali and W. P. Adams, *A Reformulation-Linearization Technique for Solving Discrete and Continuous Nonconvex Problems*. Norwell, MA, USA: Kluwer Academic, ch. 8, 1999.
[27] Y. T. Hou, Y. Shi, and H. D. Sherali, *Applied Optimization Methods for Wireless Networks*. Cambridge, U.K.: Cambridge Univ. Press, 2014.
[28] V. Tripathi, R. Talak, and E. Modiano, "Age optimal information gathering and dissemination on graphs," in *Proc. IEEE Conf. Comput. Commun. (INFOCOM)*, Apr. 2019, pp. 2422–2430.
[29] B. Yin *et al.*, "Only those requested count: Proactive scheduling policies for minimizing effective age-of-information," in *Proc. IEEE Conf. Comput. Commun. (INFOCOM)*, Apr. 2019, pp. 109–117.
[30] S. Farazi, A. G. Klein, J. A. McNeill, and D. Richard Brown, "On the age of information in multi-source multi-hop wireless status update networks," in *Proc. IEEE 19th Int. Workshop Signal Process. Adv. Wireless Commun. (SPAWC)*, Jun. 2018, pp. 1–5.
[31] A. M. Bedewy, Y. Sun, and N. B. Shroff, "The age of information in multihop networks," *IEEE/ACM Trans. Netw.*, vol. 27, no. 3, pp. 1248–1257, Jun. 2019.

Jiadong Lou (Student Member, IEEE) received the B.E. degree from the School of Computer Science and Technology, Harbin Institute of Technology, in 2018. He is currently pursuing the Ph.D. degree with the School of Computing and Informatics, University of Louisiana at Lafayette, Lafayette, LA, USA. His research interests include networking, mobile applications analysis, and network protocols security.

Xu Yuan (Member, IEEE) received the B.S. degree from the Department of Information Technology, Nankai University, Tianjin, China, in 2009, and the Ph.D. degree from the Bradley Department of Electrical and Computer Engineering, Virginia Tech, Blacksburg, VA, USA, in 2016. From 2016 to 2017, he was a Post-Doctoral Fellow of Electrical and Computer Engineering with the University of Toronto, Toronto, ON, Canada. He is currently an Assistant Professor with the School of Computing and Informatics, University of Louisiana at Lafayette, Lafayette, LA, USA. His research interests include wireless communication, networking, cyber-physical system, security, and privacy.

Sastry Kompella (Senior Member, IEEE) received the Ph.D. degree in computer engineering from Virginia Tech, Blacksburg, VA, USA, in 2006. He is currently the Section Head of the U.S. Naval Research Laboratory, Wireless Network Research Section under the Information Technology Division, Washington, DC, USA. His research interests include various aspects of wireless networks, from mobile ad hoc to underwater acoustic networks, with the specific focus towards cognitive and cooperative network optimization, programmable networking, and fundamental limits of information latency.

Nian-Feng Tzeng (Fellow, IEEE) has been with the Center for Advanced Computer Studies, School of Computing and Informatics, University of Louisiana at Lafayette, since 1987. His current research interests include the areas of high-performance computer systems, and parallel and distributed processing. He was a recipient of the Outstanding Paper Award of the Tenth IEEE International Conference on Distributed Computing Systems, in May 1990, and the University Foundation Distinguished Professor Award, in 1997. He was on the Editorial Board of the IEEE TRANSACTIONS ON PARALLEL AND DISTRIBUTED SYSTEMS, from 1998 to 2001, and on the Editorial Board of the IEEE TRANSACTIONS ON COMPUTERS, from 1994 to 1998. He was the Chair of Technical Committee on Distributed Processing, the IEEE Computer Society, from 1999 till 2002.